nature chemistry

ARTICLES

PUBLISHED ONLINE: 31 JANUARY 2010 | DOI: 10.1038/NCHEM.540

Formation of mixed-phase particles during the freezing of polar stratospheric ice clouds

Anatoli Bogdan[1,2,3]*, Mario J. Molina[4], Heikki Tenhu[2], Erwin Mayer[5] and Thomas Loerting[1]*

Polar stratospheric clouds (PSCs) are extremely efficient at catalysing the transformation of photostable chlorine reservoirs into photolabile species, which are actively involved in springtime ozone-depletion events. Why PSCs are such efficient catalysts, however, is not well understood. Here, we investigate the freezing behaviour of ternary HNO_3–H_2SO_4–H_2O droplets of micrometric size, which form type II PSC ice particles. We show that on freezing, a phase separation into pure ice and a residual solution coating occurs; this coating does not freeze but transforms into glass below ~150 K. We find that the coating, which is thicker around young ice crystals, can still be approximately 30 nm around older ice crystals of diameter about 10 μm. These results affect our understanding of PSC microphysics and chemistry and suggest that chlorine-activation reactions are better studied on supercooled HNO_3–H_2SO_4–H_2O solutions rather than on a pure ice surface.

PSCs have a crucial role in ozone depletion in the winter/spring polar stratosphere[1–3] because chlorine-activation reactions on cloud particles proceed faster than those in the gaseous phase[4,5]. According to current knowledge, PSCs can be one of three types, Ia, Ib and II, and are thought to consist of solid nitric acid trihydrate ($HNO_3{\cdot}3H_2O$ (NAT)) particles, supercooled liquid HNO_3–H_2SO_4–H_2O droplets and solid ice particles, respectively[5–7]. Type Ia and Ib PSCs are formed in the Arctic and Antarctic stratospheres. Type II PSCs are formed mainly in the cold Antarctic region below the ice frost-point of ~189 K by the homogeneous freezing of HNO_3–H_2SO_4–H_2O droplets[8] with an excess of HNO_3. Herein we deal with the formation and morphology of type II PSC ice particles. Previously it had been believed that the freezing of HNO_3–H_2SO_4–H_2O droplets led to the formation of completely solid ice particles with the acids buried within the ice phase. This belief could be because the freezing of HNO_3–H_2SO_4–H_2O droplets rich in HNO_3 of size and composition representative of the polar stratosphere takes place at temperatures much lower than the eutectic point of the HNO_3–H_2O system (~231 K). Therefore, the fate of H^+, NO_3^- and SO_4^{2-} ions during the freezing of HNO_3–H_2SO_4–H_2O droplets with an excess of HNO_3 has not been investigated before.

It was shown recently that the rate of chlorine-activation reactions may depend on the phase state of the surface of PSC ice crystals[9]. The first stage of the most important chlorine-activation reaction of $HCl + ClONO_2 \rightarrow Cl_2 + HNO_3$ (refs 2,4) is the incorporation of HCl into the ice surface with subsequent HCl ionization[2]. For the ionization of HCl about six or more H_2O molecules are needed[10,11], and so the rate of the reaction clearly depends on whether the surface of the ice is solid or coated with a quasi-liquid layer. The formation of the quasi-liquid layer through the interaction of HCl with ice was predicted[3] and also observed experimentally[9,12–14]. The chlorine-activation reactions on the surface of hexagonal ice were studied intensively, both theoretically and experimentally[6,7,9–13,15,17]. The studies were motivated by the belief, as mentioned above, that the freezing of HNO_3–H_2SO_4–H_2O droplets produces completely solid ice particles. In this Article, we present differential scanning calorimetry (DSC) results that demonstrate that during the freezing of HNO_3–H_2SO_4–H_2O droplets of size and composition representative of the polar stratosphere, H^+, NO_3^- and SO_4^{2-} ions are expelled from the ice lattice to form a residual freeze-concentrated solution that does not freeze, but transforms into glass at ~150 K (refs 18–20). Our results indicate that type II PSC ice crystals cannot be completely solid, as previously believed, but are enveloped by a supercooled HNO_3–H_2SO_4–H_2O coating.

Results

Phase behaviour of HNO_3–H_2SO_4–H_2O droplets on cooling and/or warming. Figure 1 demonstrates the phase separation into ice and a residual solution during the freezing of HNO_3–H_2SO_4–H_2O droplets. In Fig. 1, the calorimetric thermograms of emulsified 23 weight per cent (wt%) HNO_3 and 3 wt% H_2SO_4 are presented. In the thermograms, the exothermic peaks (pointing upwards) are a result of the heat of fusion released during freezing. Figure 1a demonstrates that ice is formed at ~189 K on cooling. This is inferred because the melting peak at ~248 K exactly matches the melting point of ice in the phase diagram of HNO_3–H_2SO_4–H_2O that contains 3 wt% H_2SO_4 (see Fig. 2b). In Fig. 1b, the cooling thermogram demonstrates that, after the ice has formed, the glass transition[18–20] occurs at $T_g \approx 150$ K. The appearance of the glass transition indicates that the droplets do not freeze completely. After freezing, a fraction of each droplet remains liquid until its transformation into glass. The liquid, which remains unfrozen, is a residual solution of the H^+, NO_3^- and SO_4^{2-} ions expelled from the ice lattice during freezing. The residual solution, being a viscous, fragile liquid[18,19], transforms into glass at $T_g \approx 150$ K. That the glass transition occurs at T_g much below the lowest atmospheric temperature (~183–185 K) indicates that the freshly formed PSC ice crystals can be enveloped with a residual HNO_3–H_2SO_4–H_2O coating. Previously, we reported on the formation of H_2SO_4–H_2O and H_2SO_4–HNO_3–H_2O coatings around cirrus ice crystals formed by the homogeneous freezing of H_2SO_4–H_2O

[1]Institute of Physical Chemistry, University of Innsbruck, Innrain 52a, A-6020 Innsbruck, Austria, [2]Laboratory of Polymer Chemistry, Department of Chemistry, University of Helsinki, Helsinki, PO Box 55, FIN-00014, Finland, [3]Department of Physical Sciences, University of Helsinki, Helsinki, PO Box 64, FI-00014, Finland, [4]Department of Chemistry and Biochemistry, University of California, San Diego, La Jolla, California 92093-0356, USA, [5]Institute of General, Inorganic & Theoretical Chemistry, University of Innsbruck, Innrain 52a, A-6020 Innsbruck, Austria. *e-mail: anatoli.bogdan@uibk.ac.at; thomas.loerting@uibk.ac.at

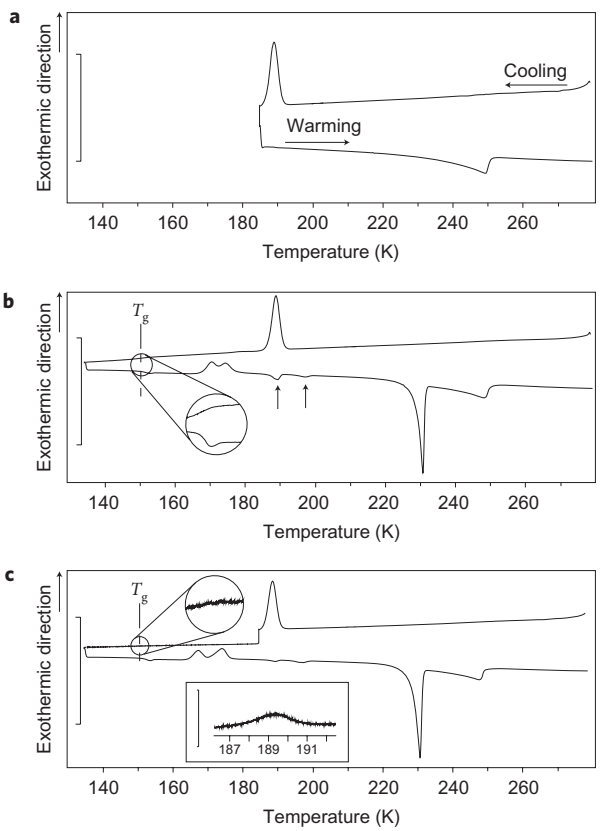

Figure 1 | DSC thermograms obtained from three samples of emulsified 23 wt% HNO_3 and 3 wt% H_2SO_4. **a**, When cooling to and warming from ~185 K at 3 K min^{-1} the exothermic and endothermic peaks obtained result from the freezing and melting of ice, respectively. **b**, When cooling to ~133 K at 3 K min^{-1} additional transitions are seen, namely a liquid-to-glass transition[18–20] on cooling and a glass-to-liquid transition on warming (magnified part). These transitions manifest themselves as a step in the corresponding thermogram[20,23]. On warming, two additional freezing events and three additional melting events are observed (see text for explanation). Arrows point to the more subtle features of the glass-to-liquid transition and to two melting endotherms. **c**, The absence of a second freezing event on cooling and the presence of the liquid-to-glass transition (magnified part) is also found for a cooling rate of 0.05 K min^{-1}, which is more relevant to the polar stratosphere. The straight line between 185 and 133 K and the thermogram in the inset were obtained at 0.05 K min^{-1}. The scale bars (0.2 W g^{-1} in main plots; 0.01 W g^{-1} in inset) indicate heat flow through the samples.

droplets[21] and H_2SO_4–HNO_3–H_2O droplets with an excess of H_2SO_4 (ref. 22). We also substantiated why the residual solution exists around ice crystals instead of in pockets within the ice[21]. In contrast to the H_2SO_4–H_2O coating and the coating of H_2SO_4–HNO_3–H_2O with an excess of H_2SO_4, which both freeze below ~183 K (refs 21–23), the HNO_3–H_2SO_4–H_2O coating with an excess of HNO_3 does not freeze, but undergoes a transition into glass at ~150 K.

Figure 1b shows that on warming, the glassy residual solution transforms at $T_g \approx 150$ K into a highly viscous liquid[23], which crystallizes at ~169 and ~173 K into ice and α-NAT, respectively. The α-NAT is thought to be metastable and converts into stable β-NAT at higher temperatures[24]. The order of crystallization events was determined from additional DSC measurements, which showed that the peak at ~169 K indeed resulted from the crystallization of ice. Further warming produced two small melting peaks at ~189 and ~197 K (arrows in Fig. 1b) and two large peaks at ~231 and ~248 K. The existence of four melting events indicates that four solids were formed on cooling and warming. As discussed above, ice surrounded by the freeze-concentrated solution melts at ~248 K, but our additional measurements reveal that other droplets with varying HNO_3 and constant H_2SO_4 concentrations also produce transitions similar to those presented in Fig. 1. The transition temperatures of these measurements are collected in Fig. 2. That the melting temperatures of ~189, ~197 and ~231 K exist for droplets of different compositions suggests that these are three eutectic melting points. (1) The temperature of ~189 K may be the eutectic melting of ice–HNO_3–H_2SO_4–H_2O (ice–ternary hydrate). However, there are contradictory reports about the existence of an HNO_3–H_2SO_4–H_2O hydrate[25]. (2) The eutectic mixture of ice–sulfuric acid tetrahydrate ($H_2SO_4 \cdot 4H_2O$ (SAT)) melts at ~197 K. In the H_2SO_4–H_2O phase diagram[26,27], the eutectic temperature of ice–SAT is ~199 K. Our lower temperature results from the presence of HNO_3. (3) The eutectic mixture of ice–NAT melts at ~231 K (ref. 25). The eutectic melting of ice–NAT decreases with increasing H_2SO_4, as shown by the dashed green line in Fig. 2b. The dashed line is a locus of the eutectics of ice–NAT in bulk HNO_3–H_2SO_4–H_2O (ref. 25). Fig. 2b also shows that the concentration along the locus is ~32 wt% $HNO_3 + H_2SO_4$. After melting of ice–NAT, the only solid that remains is ice, so the concentration of residual solution is that along the locus. For the HNO_3–H_2SO_4–H_2O droplets with 0, 3 and 6 wt% H_2SO_4 studied here, the concentration of residual solution is ~32/0, ~29/3 and ~26/6 wt% HNO_3/H_2SO_4, respectively.

The cooling rate of 3 K min^{-1} (180 K h^{-1}) is larger than that encountered in the polar stratosphere (2–80 K h^{-1} (ref. 28)). This faster cooling rate may produce a freezing temperature of ice, T_i, colder than that in the polar stratosphere[8]. It may also cause a glass transition in the residual solution, rather than freezing. It is known that T_i decreases with an increasing cooling rate[8] and the volume of a liquid determines a critical cooling rate, which ensures that freezing is avoided and brings about the glass transition[29]. Therefore, we carried out DSC measurements using a cooling rate of 0.05 K min^{-1} (3 K h^{-1}), which is similar to the synoptic temperature change[28]. In Fig. 1c, the inset demonstrates that the T_i obtained at 0.05 K min^{-1} is only ~1 K warmer than that obtained at 3 K min^{-1}. Obviously, the signal-to-noise ratio strongly decreased. The existence of the glass-to-liquid transition at $T_g \approx 150$ K in the warming thermogram in Fig. 1c implies that the residual solution undergoes the glass transition even if a cooling rate as small as 0.05 K min^{-1} is applied. To our knowledge, the finding that the glass transition occurs at such a small cooling rate is reported here for the first time. For stratospheric implications, the most important point is that the residual solution does not freeze at the same rate as the stratospheric cooling rate.

Coating of ice with a residual freeze-concentrated solution in the polar stratosphere. In Fig. 2a, the intersection of the yellow region with the experimental ice-freezing curves gives the concentration range of the droplets that would produce stable ice at polar stratospheric conditions, namely ~26–29 wt% HNO_3 for 0 wt% H_2SO_4 and ~23–25 wt% HNO_3 for 3 wt% H_2SO_4. For simplicity, we calculated the thickness of the coating formed around ice crystals immediately after the freezing of 26–29 wt% HNO_3 droplets. The presence of a small amount of H_2SO_4 only slightly changed the thickness of the coating. We showed (see above) that after freezing HNO_3–H_2O droplets, the residual solution was about ~32 wt% HNO_3. We assumed that the diameter of HNO_3–H_2O droplets is 0.4–2.4 μm and that freshly formed ice crystals are spherical with a smooth surface. In fact, as our optical microscopy observations show, the surface of ice is slightly rough (Fig. 3a). The assumption is justified because observation of cold cirrus clouds, which are formed near the tropopause region at similar conditions as PSCs, reveal quasi-spherical ice crystals of

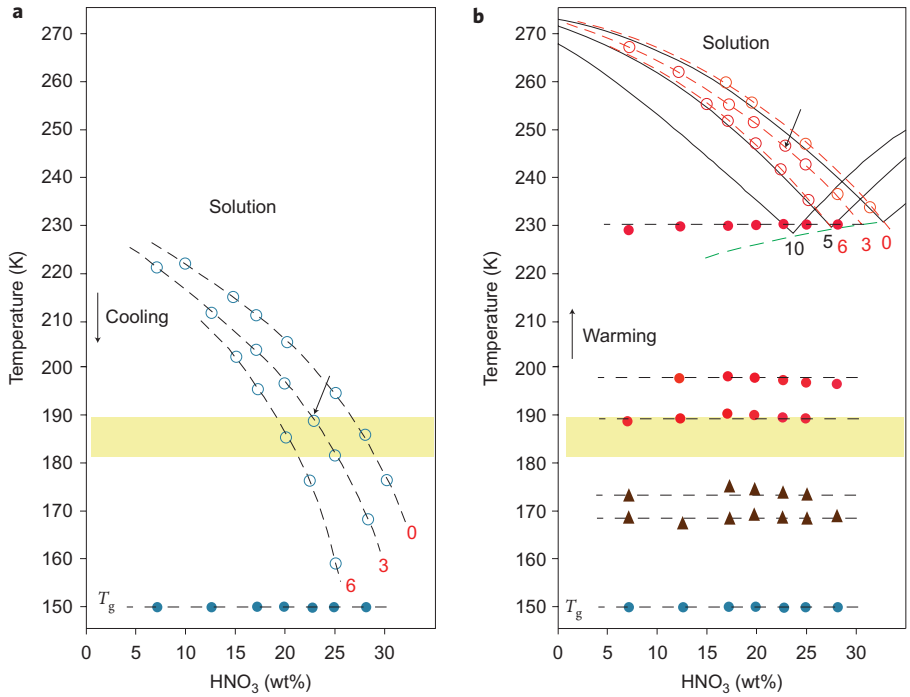

Figure 2 | The transition temperatures for the cooling and warming of bulk[25] and emulsified HNO_3–H_2SO_4–H_2O. a, The transition temperatures obtained on cooling. The red numbers denote wt% H_2SO_4 in the emulsified HNO_3–H_2SO_4–H_2O. The open and filled blue circles are the freezing and glass-transition points of emulsified HNO_3–H_2SO_4–H_2O. **b**, The transition temperatures obtained on warming. The red and black numbers denote wt% H_2SO_4 in the emulsified and bulk HNO_3–H_2SO_4–H_2O, respectively. The black solid lines are the phase diagrams of bulk HNO_3–H_2SO_4–H_2O (ref. 25). The green dashed line is a locus of the eutectics of bulk HNO_3–H_2SO_4–H_2O (ref. 25). The open red circles are the melting points of ice in emulsified HNO_3–H_2SO_4–H_2O. The solid red circles are the eutectics of ice–NAT (~231 K), ice–SAT (~197 K) and ice–ternary hydrate (~189 K) of the emulsified HNO_3–H_2SO_4–H_2O with 3 wt% H_2SO_4. The black triangles denote the cold crystallizations that occur on warming the emulsified HNO_3–H_2SO_4–H_2O with 3 wt% H_2SO_4 (see Fig. 1). In both (**a**) and (**b**) the arrows show the freezing and melting points of ice in the thermograms in Fig. 1. The yellow field is the temperature region of the stability of ice at the polar stratospheric conditions: 50 mbar pressure and a water mixing ratio of 5 parts per million by volume H_2O (ref. 5). Error bars are smaller than the size of the symbols.

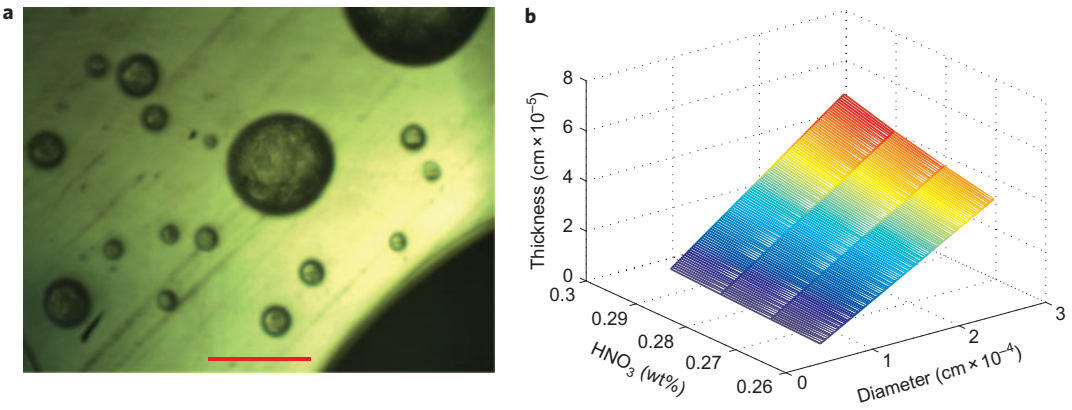

Figure 3 | Liquid coating around ice crystals. a, Microscopy image of mixed-phase particles (an ice core plus a solution coating) formed from 23/3 wt% HNO_3/H_2SO_4 droplets placed on a hydrophobic silicon surface. The picture was taken during warming at $T = \sim 235$ K immediately after eutectic ice–NAT melting (see Fig. 1b). Scale bar = 50 μm. **b**, The initial thickness of the ~32 wt% HNO_3 coating that would envelop spherical ice crystals after freezing of 26–29 wt% HNO_3 droplets of diameter 0.4–2.4 μm.

diameter <65 μm (ref. 30). We found that HNO_3–H_2O droplets produced an initial coating ~80–600 nm thick (Fig. 3b).

Discussion

We have demonstrated that droplets of micrometric size experience a phase separation into pure ice and a residual freeze-concentrated solution at temperatures, chemical compositions and cooling rates relevant to the polar stratosphere. Freeze-concentrated, HNO_3-rich ternary solutions do not freeze on continued cooling, but rather transform into a freeze-concentrated glass, in contrast to H_2SO_4-rich ternary solutions. As seen in the microscopy image in Fig. 3a, the liquid is expelled from the ice and coats it rather than being incorporated within the ice (for example, in pockets).

In the stratosphere, the surface of the outer coating equilibrates rapidly with the environment to reach the composition of freezing droplets. The inner surface of the coating remains in equilibrium

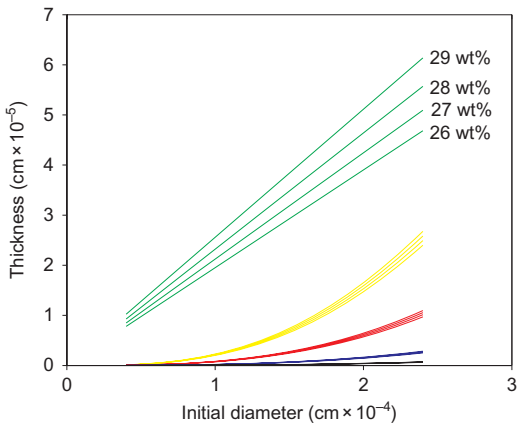

Figure 4 | Thickness of the ice crystal coating. The thickness of the coating that would envelop young and aged PSC ice crystals for four concentrations of HNO_3 in droplets from which the ice crystals formed. The green lines show the thicknesses of the initial coating (Fig. 3). The yellow, red, blue and black lines are the thicknesses of the coating around the aged ice crystals grown to diameters of 3, 5, 10 and 20 μm, respectively.

with the ice core, and thus preserves the composition of ~32 wt% HNO_3. As a result of the concentration gradient, H_2O molecules on the surface diffuse through the coating and become incorporated into the ice. Assuming that the volume of the coating is limited by the acid content, the coating becomes thinner as the ice crystals grow. Ice PSC crystals can reach a diameter of ~10 μm (ref. 5). We calculated that the coating around such ice crystals would be ~30 nm thick (Fig. 4). In fact, the coating could be thicker because of the reactions of gaseous NO_y (ref. 6) and HCl (refs 11–13) with liquid H_2O. The reactions produce the condensed-phase HNO_3 (ref. 6) which, together with the additionally condensed H_2O, increases the volume of the coating and consequently its thickness. With time, as the amount of the condensed-phase HNO_3 increases, the coating may become almost binary HNO_3–H_2O. Thus, our results indicate that chlorine-activation reactions on type II PSC ice crystals, which finally results in polar stratospheric ozone depletion in springtime, can be governed by supercooled HNO_3–H_2SO_4–H_2O or HNO_3–H_2O solutions rather than by the pure ice surface. The coating may prolong the lifetime of ice crystals by suppressing their evaporation above ~189 K (ref. 24), which can account for the presence of ice crystals in the polar stratosphere at temperatures above 189 K (ref. 31).

Methods

We prepared HNO_3–H_2SO_4–H_2O solutions that contained 7–32 wt% HNO_3 and 0, 1, 3, 4 and 6 wt% H_2SO_4 by mixing 95–97 wt% H_2SO_4 and 65 wt% HNO_3 (Riedel-de Haën, Germany) with the corresponding amount of ultra-pure deionized water. Titration of HNO_3–H_2O solutions against standard 2N NaOH showed an accuracy of ±0.1 wt%. The oil phase used to form the emulsion was prepared by using 80 wt% Halocarbon 0.8 oil (Halocarbon Products Corp.) and 20 wt% lanolin (Sigma Aldrich). The oil phase and solution-in-oil emulsions were prepared according to the method of Chang *et al.* (ref. 8). The diameter of the droplets in the emulsions was measured with an optical microscope and found to be <5 μm. In Fig. 2, only the experimental data for the droplets of composition 7–32 wt% HNO_3 and 0, 3 and 6 wt% H_2SO_4 are presented.

The calorimetric measurements of the emulsion samples were carried out with a Mettler Toledo DSC822. The calorimeter is well calibrated and reproduced the melting points of indium (429.75 K), water (273.15 K) and heptane (~182 K) with an accuracy of ±0.4 K. The weight of the emulsion samples was ~25–35 mg. The DSC measurements were performed between 133 and 278 K at scanning rates of 3 and 0.05 K min^{-1}.

The oil-phase environment does not induce heterogeneous freezing of the droplets. This conclusion is inferred from a number of DSC measurements that showed emulsified, pure-water droplets always freeze at a homogeneous freezing temperature of $T_h \approx 233$ K. Chang *et al.* provide estimations of the stability of lanolin[8], and showed no appreciable reaction between lanolin and concentrated H_2SO_4–H_2O and HNO_3–H_2O on a time scale of two days[8]. Nevertheless, to prevent any degradation of lanolin, we made all DSC measurements in less than two hours from the moment of contact between the solutions and the oil phase. Repeated measurements performed for each composition of emulsified droplets showed very good reproducibility of the transition temperatures.

Received 12 November 2009; accepted 18 December 2009; published online 31 January 2010

References

1. Solomon, S., Garcia, R. R., Rowland, F. S. & Wuebbles, D. J. On the depletion of Antarctic ozone. *Nature* **321,** 755–758 (1986).
2. Molina M. J., Tso, T. L., Molina, L. T. & Wang, F. C. Y. Antarctic stratospheric chemistry of chlorine nitrate, hydrogen chloride, and ice: release of active chlorine. *Science* **238,** 1253–1257 (1987).
3. Molina, M. J. in *The Chemistry of the Atmosphere: The Impact of Global Change* (ed. Calvet, J. G.) 27–38 (Blackwell, 1994).
4. Molina, M. J., Molina, L. T. & Golden, D. M. Environmental chemistry (gas and gas–solid interactions): the role of physical chemistry. *J. Phys. Chem.* **100,** 12888–12896 (1996).
5. Prenni, A. J. & Tolbert, M. A. Studies of polar stratospheric cloud formation. *Acc. Chem. Res.* **34,** 545–553 (2001).
6. Zondlo, M. A., Barone, S. B. & Tolbert, M. A. Condensed-phase products in heterogeneous reactions: N_2O_5, $ClONO_2$, and HNO_3 reacting on ice films at 185 K. *J. Phys. Chem. A* **102,** 5735–5748 (1998).
7. Zondlo, M. A., Hudson, P. K., Prenni, A. J. & Tolbert, M. A. Chemistry and microphysics of polar stratospheric clouds and cirrus clouds. *Ann. Rev. Phys. Chem.* **51,** 473–499 (2000).
8. Chang, H.-Y. A., Koop, T., Molina, L. T., & Molina, M. J. Phase transitions in emulsified HNO_3/H_2O and $HNO_3/H_2SO_4/H_2O$ solutions. *J. Phys. Chem. A* **103,** 2673–2679 (1999).
9. Buesnel, R., Hillier, I. H. & Masters, A. J. Molecular dynamics simulation of the ionization of hydrogen chloride in water clusters using a quantum mechanical potential. *Chem. Phys. Lett.* **247,** 391–394 (1995).
10. Pursell, C. J., Zaidi, M., Thompson, A., Franser-Caston, C. & Vela, E. Acid–base chemistry on crystalline ice: HCl + NH_3. *J. Phys. Chem. A* **104,** 552–556 (2000).
11. McNeil, V. F., Loerting, T., Geiger, F. M., Trout, B. L. & Molina, M. J. Hydrogen chloride-induced surface disordering on ice. *Proc. Natl Acad. Sci. USA* **103,** 9422–9427 (2006).
12. McNeill, V. F. *et al.* Interaction of hydrogen chloride with ice surfaces: the effects of grain size, surface roughness, and surface disorder. *J. Phys. Chem. A* **111,** 6274–6284 (2007).
13. Fluckiger, B., Chaix, L. & Rossi, M. J. Properties of the HCl/ice, HBr/ice, and H_2O/ice interface at stratospheric temperatures (200 K) and its importance for atmospheric heterogeneous reactions. *J. Phys. Chem. A* **104,** 11739–11750 (2000).
14. Bogdan, A., Kulmala, M., MacKenzie, A. R. & Laaksonen, A. Study of finely divided aqueous systems as an aid to understanding the surface chemistry of polar stratospheric clouds: case of HCl/H_2O and HNO_3/HCl/H_2O systems. *J. Geophys. Res.* **108,** 4303, doi:10.1029/2002JD002606 (2003).
15. Oppliger, R., Allanic, A. & Rossi, M. J. Real-time kinetics of the uptake of $ClONO_2$ on ice and in the presence of HCl in the temperature range 160 K ≤ *T* ≤ 200 K. *J. Phys. Chem. A* **101,** 1903–1911 (1997).
16. Gertner, B. J. & Hynes, J. T. Molecular dynamic simulation of hydrochloric acid ionization at the surface of stratospheric ice. *Science* **271,** 1563–1565 (1996).
17. Wofsy, S. C., Molina, M. J., Salawitch, R. J., Fox, L. E. & McElroy, M. B. Interactions between HCl, NO_x, and H_2O ice in the Antarctic stratosphere: implication for ozone. *J. Geophys. Res.* **93,** 2442–2450 (1988).
18. Angell, C. A. The old problems of glass and the glass transition, and the many new twists. *Proc. Natl Acad. Sci. USA* **92,** 6675–6682 (1995).
19. Angell, C. A. Formation of glasses from liquids and biopolymers. *Science* **267,** 1924–1935 (1995).
20. Debenedetti, P. G. & Stillinger, F. H. Supercooled liquids and the glass transition. *Nature* **410,** 259–267 (2001).
21. Bogdan, A., Molina, M. J., Sassen, K. & Kulmala, M. Formation of low-temperature cirrus from H_2SO_4/H_2O aerosol droplets. *J. Phys. Chem. A* **110,** 12541–12542 (2006).
22. Bogdan, A. & Molina, M. J. Why does large relative humidity with respect to ice persist in cirrus ice clouds? *J. Phys. Chem. A* **113,** 14123–14130 (2009). doi: 10.1021/jp9063609.
23. Bogdan, A. Reversible formation of glassy water in slowly cooling diluted drops. *J. Phys. Chem. B* **110,** 12205–12206 (2006).
24. Delval, C. & Rossi, M. J. Influence of monolayer amounts of HNO_3 on the evaporation rate of H_2O over ice in the range 179 to 208 K: a quartz crystal microbalance study. *J. Phys. Chem. A* **109,** 7151–7165 (2005).
25. Beyer, K. D., Hansen, A. R. & Raddatz, N. Experimental determination of the $H_2SO_4/HNO_3/H_2O$ phase diagram in regions of stratospheric importance. *J. Phys. Chem. A* **108,** 770–780 (2004).

26. Beyer, K. D., Hansen, A. R. & Poston, M. The search for sulfuric acid octahydrate: experimental evidence. *J. Phys. Chem. A* **107,** 2025–2932 (2003).
27. Gable, C. M., Betz, H. F. & Maron, S. H. Phase equilibria of the system sulfur trioxide–water. *J. Am. Chem. Soc.* **72,** 1445–1448 (1950).
28. Carslaw, K. S. *et al*. Particle microphysics and chemistry in remotely observed mountain polar stratospheric clouds. *J. Geophys. Res.* **103,** 5785–5796 (1998).
29. Macfarlane, D. R. Continuous cooling (CT) diagrams and critical cooling rates: a direct method of calculations using the concept of additivity. *J. Non-Cryst. Solids* **53,** 61–72 (1982).
30. Lawson, R. P. *et al*. Aircraft measurements of microphysical properties of subvisible cirrus in the tropical tropopause layer. *Atmos. Chem. Phys.* **8,** 1609–1620 (2008).
31. Deshler, T., Peter, T., Müller, R. & Crutzen, P. The lifetime of leewave-induced ice particles in the Arctic stratosphere: I. Balloonborne observations. *Geophys. Res. Lett.* **21,** 1327–1330 (1994).

Acknowledgements

We thank E. Bertel, S.C. Wofsy and M.B. McElroy for discussions. A.B. thanks the Physical and Chemical Departments of the University of Helsinki for providing facilities to perform the experiments. We are grateful for financial support from the European Research Council (Starting Grant SULIWA) and the Austrian Science Fund (START award Y391).

Author contributions

A.B. designed the study, performed measurements and calculations, collected and analysed data, and wrote the manuscript. M.J.M. designed the study, analysed data, and wrote and corrected the manuscript. H.T., E.M. and T.L. analysed data, and wrote and corrected the manuscript. All authors discussed the results and commented on the manuscript.

Additional information

The authors declare no competing financial interests. Reprints and permission information is available online at http://npg.nature.com/reprintsandpermissions/. Correspondence and requests for materials should be addressed to A.B. and T.L.